LAWRENCE
LIVERMORE
NATIONAL
LABORATORY

LLNL-PROC-565933

Microarcsecond relative astrometry from the ground with a diffractive pupil

S. M. Ammons, E. Bendek, O. Guyon, B. Macintosh, D. Savransky

July 24, 2012

SPIE Astronomical Telescopes and Instrumentation
Amsterdam, Netherlands
July 1, 2012 through July 6, 2012

Disclaimer

Theoretical Limits on Bright Star Astrometry with Multi-Conjugate Adaptive Optics using a Diffractive Pupil

S. Mark Ammons*[a], Eduardo A. Bendek[b], Olivier Guyon[b,c], Bruce Macintosh[a], Dmitry Savransky[a]

[a]Lawrence Livermore National Laboratory, Physics Division, L-210, 7000 East Ave., Livermore, CA USA 94550
[b]Steward Observatory, University of Arizona, 933 Cherry Ave, Tucson, AZ USA 95060
[c]Subaru Telescope, 640 N. Aohoku Place, Hilo, HI, US

ABSTRACT

We present a ground-based technique to detect or follow-up long-period exoplanets via precise relative astrometry of host stars using Multi-Conjugate Adaptive Optics (MCAO) on 8 meter telescopes equipped with diffractive masks. MCAO improves relative astrometry by sharpening PSFs, reducing the star centroiding error, and by providing a spatially stable, more easily modeled PSF. However, exoplanet mass determination requires multi-year reference grid stability of ~10-100 uas or nanometer-level stability on the long-term average of out-of-pupil phase errors, which is difficult to achieve with MCAO. The diffractive pupil technique calibrates dynamic distortion via extended diffraction spikes generated by a dotted primary mirror, which are referenced against a grid of background stars. We calculate the astrometic performance of a diffractive 8-meter telescope with diffraction-limited MCAO in *K* using analytical techniques and a simplified MCAO simulation. Referencing the stellar grid to the diffraction spikes negates the cancellation of Differential Tip/Tilt Jitter normally achieved with MCAO. However, due to the substantial gains associated with sharper, more stable PSFs, diffractive 8-m MCAO reaches ~ 4-6 μas relative astrometric error per coordinate in one hour on a bright target star (K ~ 7) in fields of moderate stellar density (~10 stars arcmin^{-2}). Final relative astrometric precision with MCAO is limited by atmospheric differential tip/tilt jitter.

Keywords: astrometry, diffractive pupil, microarcsecond, SIM, PECO, differential atmospheric refraction, extrasolar planet, exoearth, differential tip/tilt jitter, MCAO, adaptive optics

1. INTRODUCTION

1.1 Science with Microarcsecond Astrometry

Astrometry, or the measurement of positions of astrophysical objects, is a technology in which great developments are yet to be made to reach the theoretical limits of precision.[1] The ability to measure the relative positions of objects at the microarcsecond level would be a fundamentally new tool that could be applied to a range of science areas: Earth and exoplanet detection and characterization, Galactic and halo structure, the physics of supermassive black holes and accretion, and stellar astrophysics.

1.1.1. Astrometry for Exoplanet Detection and Orbit Measurement. Both the astrometric signature of an orbiting exoplanet and the contrast-limited sensitivity of direct imaging increase with the separation of the planet from its host star. Thus, astrometry and direct imaging combine to yield full orbit parameters and exoplanet masses with significant overlap between samples.[2,3] Astrometry is complementary to well-developed radial velocity techniques, which are more sensitive to small star-planet separations.[4] Since many direct imaging surveys specifically target young stars with active chromospheres and thus large radial velocity jitter, astrometric follow-up techniques compare favorably to Doppler follow-up (Figure 1).

*ammons1@llnl.gov; phone 1 925 422-2102; www.u.arizona.edu/~ammons81/

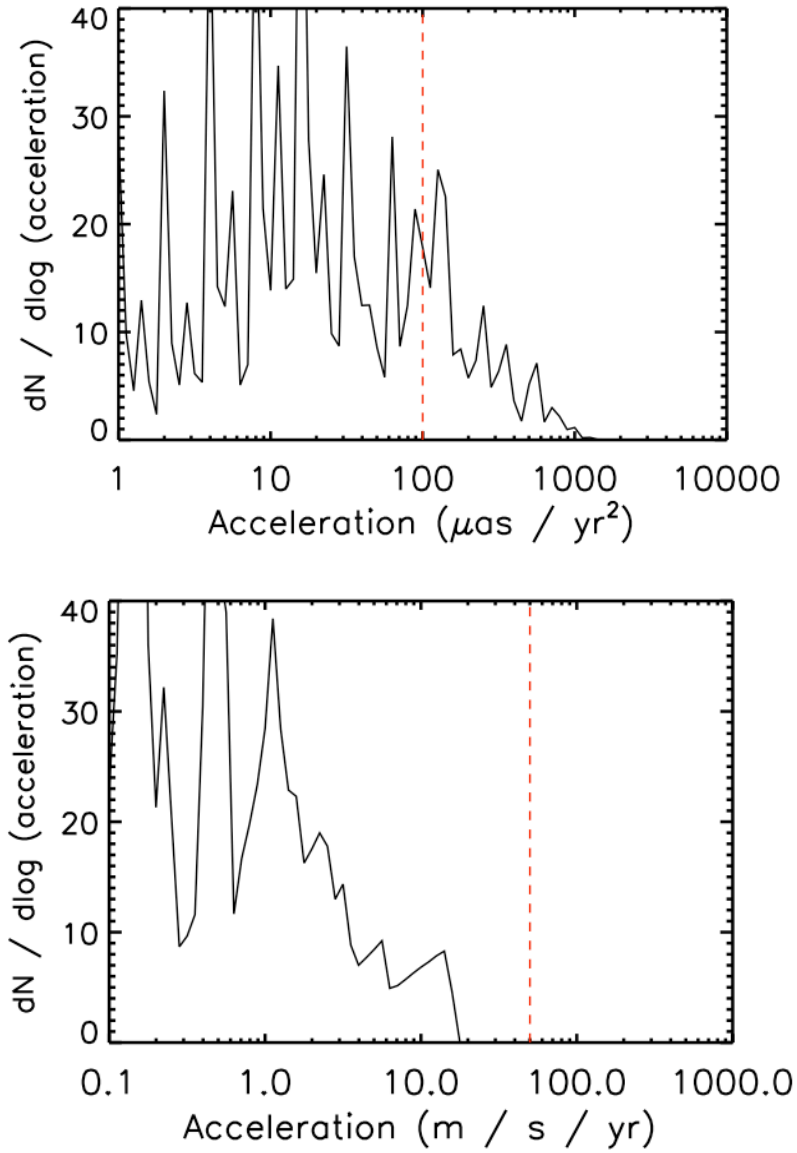

Fig. 1. *Top panel:* Histogram of astrometric star acceleration for simulated suite of planetary orbits consistent with detection by the Gemini Planet Imager[5] (modified by D. Savransky, priv. comm.). Units are in microarcseconds per year^2. The red dashed line marks approximately the acceleration detectable in one year with the best single-epoch relative astrometric precision currently available, obtained in the crowded Galactic Center on the Keck AO system.[6] A substantial fraction of the detected population has acceleration measurable with astrometric techniques. *Bottom panel:* Histogram of Doppler star acceleration for the same simulated suite of planetary orbits. Units are in meters per second per year. The red dashed line marks approximately the acceleration detectable in one year using Doppler techniques, assuming 50 m s^{-1} astrophysical jitter, as expected for young stars. Notice that jitter smaller than 20 m s^{-1} is required for any target to have measurable acceleration.

1.1.2. *Astrometry for Science Beyond the Local Neighborhood.* Combined with radial velocities, microarcsecond astrometry with large telescopes (D ≥ 5 meters) would yield the 3D position and space motions of individual red giants in the Galactic halo, which could constrain models of Galactic structure and the distribution of dark matter within our Galaxy and in local dwarf galaxies.[7] Beyond our Galaxy, precise astrometry can probe the time variability of the photocenters of nearby quasars and Active Galactic Nuclei (AGN), potentially revealing the space density of binary

supermassive black holes and constraining models of the morphology and cloud distribution within the compact optical emission in their central engines.[8]

1.2. Systematic Errors Limit Astrometric Precision with Ground-Based Telescopes

State-of-the-art astrometric precision has seen significant improvement in the last 15 years, with the exploitation of extensive calibration (reaching ~100 μas),[9] high resolution from space (HST Fine Guidance Sensor,[10] and HIPPARCOS,[11] ~1 mas precision), adaptive optics (Palomar[12] and Keck AO[6], reaching to 100-300 μas), and small-aperture interferometers (Palomar Test Interferometer[13], ~20 μas). Although GAIA will reach a final mission precision of better than 20 μas for bright stars,[14] it is not targeted and will not optimize observational cadence for individual stars. Despite the clear advantages of space telescopes for astrometry, most technological developments in this field have been made from the ground in the past decade.

Astrometric precision improves drastically as telescope diameter increases, and extremely large telescopes are predicted to deliver precisions of ~1-10 μas if systematic errors can be addressed,[15,16,17] nearly two orders of magnitude better than currently possible. Like radial velocity work in the 1980's before the refinement of the iodine cell technique,[18,19] astrometry has been limited to the ~100 μas level by numerous systematic errors that must be tackled individually it can be fully exploited.[1]

1.3. Addressing Limiting Systematic Errors with the Diffractive Pupil

1.3.1. *Calibrating dynamic distortion with the diffractive pupil.* A diffractive pupil has been proposed to calibrate dynamic distortion changes introduced by the instrument in real time for narrow-angle, bright star astrometry.[20,21,17] In this method, a series of imprinted dots or a mask with small, ~1 mm holes is introduced into the beam above the primary mirror, inducing diffraction spikes from a central, bright target star. Similar to the iodine cell's role in calibrating dynamic wavelength shifts with a standard series of lines, the technique calibrates astrometric distortion in the focal plane during an observation with a straight-line ruler created by diffraction. This technique has been implemented on a testbed at the University of Arizona for space-based platforms.[22] *The diffractive pupil is predicted to decrease this critical systematic error to the microarcsecond level* while avoiding expensive, restrictive requirements on telescope and instrument stiffness.

1.3.2. *Astrometry with Multi-Conjugate Adaptive Optics*. Adaptive optics (AO) is the technique of using deformable mirrors to rapidly (~1 kHz) correct atmospheric phase errors. The field of view of correction can be enhanced with multiple deformable mirrors in an architecture called Multi-Conjugate Adaptive Optics (MCAO), discussed further in section 2.

Narrow-angle, bright star astrometry benefits greatly from MCAO in the following ways:

1. The spatially uniform point spread functions (PSF) delivered by wide-field, MCAO systems reduce star centroiding errors resulting from inaccurate PSF models;
2. The wider fields available with MCAO include more stars in and increase the overall signal-to-noise of the reference grid of background stars;
3. The sharper PSF delivered with MCAO decreases the measurement error term;
4. *MCAO cancels differential tip/tilt jitter (DTTJ) induced by atmospheric motions* in the high atmosphere, typically the dominant astrometric error for short exposures.

1.3.3. Dynamic Optical Distortion in MCAO. For the reasons listed above, MCAO is a promising tool for narrow-field astrometry. In particular, the presence of deformable mirrors conjugated out of the pupil plane allows the freedom to actively cancel the contributions of high altitude layers to the field distortion. However, with this advantage comes the potential to systematically change the distortion on long time scales with these same mirrors. To achieve microarcsecond relative astrometry with MCAO systems on large telescopes, the long-term average of out-of-pupil phase errors must be constant at the ~nm level on year-long timescales.

Here, we explore the idea that the diffractive pupil could serve as a long-term astrometric calibrator for MCAO systems. The goal of this paper is to calculate the theoretical astrometric precision possible using an MCAO system on an 8-meter telescope equipped with a diffractive pupil.

2. SIMULATIONS OF ASTROMETRY WITH MCAO

We now attempt to calculate the astrometric performance of an MCAO system on an 8-meter telescope using a diffractive pupil, focusing on wide field cases targeting bright, on-axis stars (V < 10) and referencing to a grid of background stars (N > 5). More details about the simulations and star weighting techniques used in this paper may be found in Ammons et al. (2011).[17]

2.1 Relevant Astrometric Error Budget Terms

2.1.1. Differential Tip/Tilt Jitter. Differential Tip/Tilt Jitter (DTTJ) refers to errors in the ability to measure the angular distances between stars due to random phase fluctuations in the atmosphere. These errors are tightly correlated with the strength of upper-altitude layers in the atmosphere, which introduce distortions in the focal plane (as opposed to phase errors in the pupil plane). DTTJ error increases rapidly as a function of star separation until an angle D/h is reached, with D equal to the telescope diameter and h the height of the dominant layer of turbulence, at which point the DTTJ error asymptotes. A theoretical model for the strength of DTTJ as a function of telescope diameter and star separation is obtained from Sasiela (2007)[23] and described in more detail in Ammons et al. (2011)[17]. The Sasiela DTTJ is assumed to average down with the square root of the integration time, i.e., $\sqrt{\tau/t}$, where τ is the amount of time required for the wind to fully cross the pupil of the telescope.[8]

2.1.2. Star S/N. The theoretical best centroiding precision of star images depends on the signal to noise ratio of their detection. For a circular Point Spread Function (PSF) well-approximated by a Gaussian with a full width at half maximum of s, the theoretical limit to the centroiding precision is

$$\sigma = s / SNR$$

where SNR is the signal-to-noise ratio of the detection. This equation assumes that the star image is better than Nyquist sampled.

2.1.3. Differential Atmospheric Refraction. The atmosphere acts as a prism, diffracting light along a vector pointing to the zenith. The amount of angular motion is dependent on the wavelength of the light. This introduces a *chromatic* effect in which the apparent centroid of a particular star depends on its spectral energy distribution. For these simulations, we assume that the Gubler and Tytler (1998)[24] method is being applied, in which ground layer pressure and temperature and knowledge of star color are used to construct an atmospheric model that predicts the chromatic differential atmospheric refraction (CDAR). This model requires knowledge of the zenith position to ~36″, the ground temperature to ~0.6 K, the ground pressure to 1.6 mB, the relative humidity to ±10%, and the temperature of both stars to ~100 K to reduce the CDAR error to ~100 microarcseconds for K-band observations at a zenith angle of $\xi = 30^\circ$. This method is currently employed to reduce astrometric error due to CDAR in observations of the Galactic center.[6,25] CDAR can be reduced to the microarcsecond level with the use of narrow-band filters.[12]

The achromatic term (ADAR) is related to the difference in zenith angle between two stars being referenced. For a field of a given size, the ADAR can be fitted with third-order polynomials and removed at the sub-microarcsecond level for near-infrared (IR) observations.

2.1.4. Pixel Sampling and Crowding Errors. Sub-sampling the star PSFs can lead to "pixel-phase" errors, in which the measured centroid is dependent on the exact position of the star within a pixel.[26] Pixel phase errors can be reduced to negligible values by critically sampling the PSF.[16] The simulations we make assume the use of wide-field reference grids in which crowding error is not significant. Further information regarding assumptions made about pixel sampling is in Section 2.3.5 of Ammons et al. (2011)[17].

2.2 Simplified MCAO Simulations

2.2.1. Simulation Geometry. We now use a simple simulation to understand the distortion introduced by an idealized MCAO system on an 8-meter telescope. We assume a geometry similar to the Gemini South GEMS MCAO system[27] with 3 deformable mirrors conjugate to 0, 4.5, and 9 km altitude. The constellation 5 laser guide stars in a "quincunx" format with a constellation diameter of 120" and a Sodium excitation altitude of 90 km. A 6-layer Cerro Pachon C_N^2 with r_0 = 16 cm at 500 nm and 20 m s^{-1} wind is assumed. The simulation ignores the details of wavefront sensing and reconstruction, but simply sets DM phases equal to the inverse sum of the nearest conjugate layers. With these settings, the simulation will model the effects of fitting error and generalized anisoplanatism, but will ignore other terms like delay, bandwidth, aliasing, LGS elongation error, and tip/tilt error.

We model a diffractive pupil as a grid of crisscrossed straight rods of 1 mm diameter and 4 cm spacing. The target star is assumed to be a K = 4 star and the star reference grid is determined randomly according to the Bahcall & Soneira (1980)[28] star count model as provided in the fortran "BSGmodel" code for a Galactic latitude of 5 degrees. Example K-band Field PSFs for a 1 second integration time are shown in Figure 2.

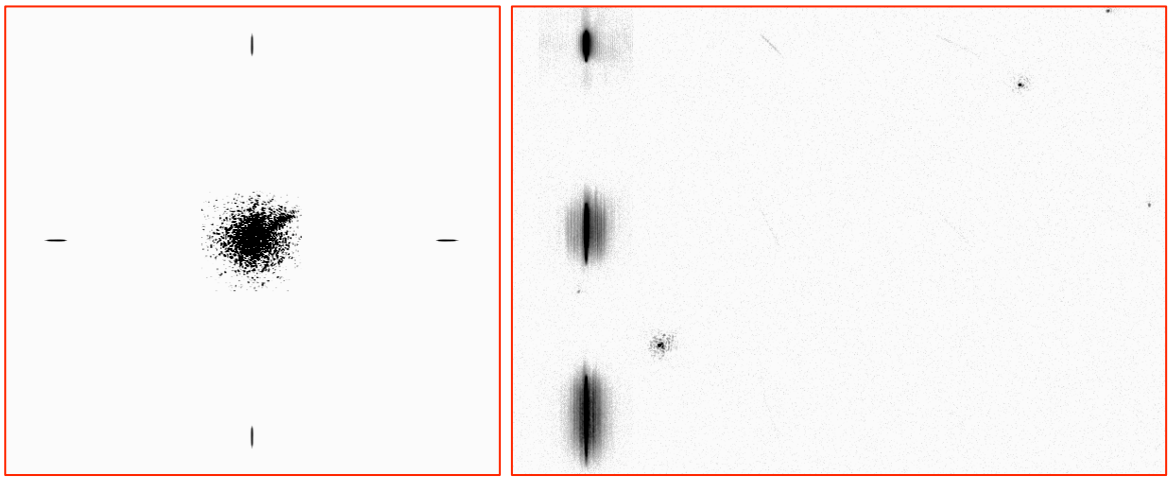

Fig. 2. Left panel: 25" x 25" field of view for an 8-m MCAO simulation centered on the K=4 target star. The focal plane is diffraction-limited at 70% Strehl in K over the full 2' field of view in this simulation. The first order diffraction spikes generated by the K=4 star are seen at the edges of the panel. *Right panel:* Off-axis 25"x40" image of first, second, and third-order diffraction spikes generated by target star. Faint diagonal diffraction spikes and five other field reference stars are also apparent.

2.2.2. Tilt Anisokineticism in MCAO with Diffractive Pupil. We now use this simulation to assess the astrometric error in the measurement of the distance between two stars as a function of exposure time. Instead of centroiding stars, which would include errors due to pixel sampling and PSF modeling, we fit the tip/tilt component of the wavefront for each star and diffraction spike in the image.

Figure 3 plots the measured tilt anisokineticism perpendicular to the separation vector between star / spike pairs at an average separation of 10". The average separation between the reference star and the target star is 48". These results are averaged over 30 atmospheric realizations of 400 seconds in length each. Note that the astrometric precision drops faster than the square root of the exposure time, as has been found in other similar simulations of tilt anisokineticism for a 30-meter telescope assuming Taylor frozen flow of Kolmogorov turbulence (B. Ellerbroek, priv. comm.). Notice that the simulated curve is closer to the theoretical DTTJ value for the full seeing predicted from the Sasiela (2007)[23] equation for a star separation of 48" (the average separation between the target star and the reference star) than 10" (the average separation between the target star and the nearest diffraction spike). This implies that the DTTJ error in the system is the same as in a seeing-limited case *without* the diffractive pupil in place.

2.2.3. Diffractive Pupil Negates Cancellation of DTTJ error. This result can be understood by considering the correlations of wavefronts seen by the target stars and the diffraction spikes. Zeroth-order light from the target star sees the on-axis wavefront from the atmosphere and the on-axis correction from the MCAO mirrors, resulting in a well-corrected PSF. Diffracted light from the target stars sees the on-axis wavefront but sees the *off-axis* correction from the MCAO mirrors, resulting in a PSF with full anisoplanatism and anisokineticism as determined by the target star-spike

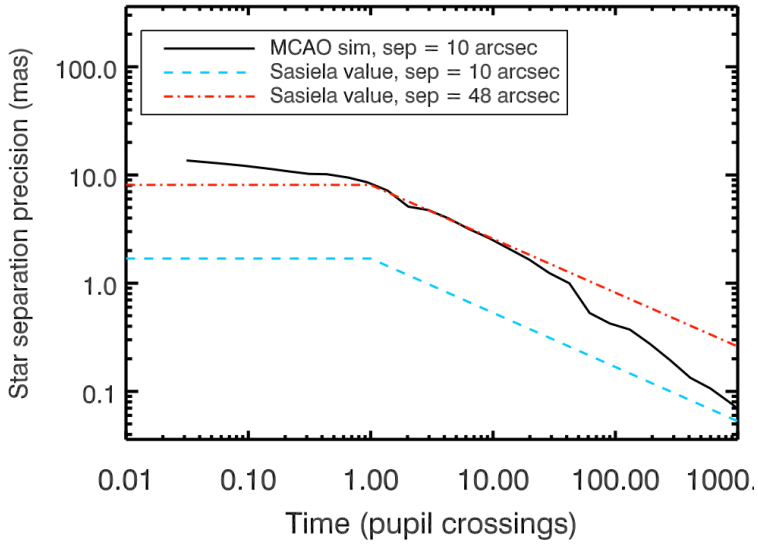

Fig. 3. Astrometric error in the distance measurement between two stars as a function of integration time. Only the component of the error perpendicular to the separation vector is plotted. The vertical unit is milliarcseconds and the exposure time is in units of pupil crossings. The black solid line is taken from the MCAO simulation described in Section 2.2 for the separation between a diffraction spike and a star located 10 arcseconds away from the spike (and 48 arcseconds away from the central star). The blue dashed line shows the theoretical DTTJ prediction from Sasiela (2007)[23] for a star separation of 48" and the red line shows the Sasiela prediction for a star separation of 10". Notice that the simulated values are closer to the theoretical value for a 48" distance than a 10" distance.

separation (average of 48" in the simulation above). Zeroth-order light from reference stars sees the off-axis wavefront of the atmosphere and the corresponding off-axis wavefront from the MCAO mirrors, resulting in a well-corrected PSF. In the end, the corrected PSFs and tilt components of the on-axis target star and the off-axis reference stars are similar, but the corrected PSFs and tilt components of the diffraction spikes and the off-axis reference stars are decorrelated. Thus, using the diffraction spikes as references causes the full seeing-limited DTTJ error to enter the system, effectively ignoring the MCAO system's cancellation of the DTTJ.

2.3 Covariance-Based Weighting Method

As the DTTJ in an MCAO + diffractive pupil combination is no different from a seeing-limited system, we turn to an analytical description of the astrometric error terms to assess the final system performance.

We model the reference star grid with the Bahcall & Soneira (1980)[28] star count model. These models are interpolated as described in Section 2.1 of Ammons et al. (2011). For a simulated circular field of view of diameter d at a Galactic latitude b, reference stars are inserted in random locations in the field according to the Bahcall & Soneira probability distribution. The telescope is circular with a 30% throughput and a 10% secondary obscuration. K-band observations are assumed. We assume 0.8″ total seeing and a sky background of K = 14 Vega magnitudes per square arcsecond. The detector is assumed to be Nyquist sampled.

The exposure time of individual frames within a total exposure is set to 3 seconds. Field stars that exceed pixel counts of 50,000 electrons in this exposure time are removed from the reference grid. Larger telescopes lose significant numbers of stars from the bright end of the reference grid to saturation.

We adopt the star weighting technique of Cameron, Britton, & Kulkarni (2009)[12] to minimze the final astrometric motion of the target star relative to the reference grid with respect to the theoretical covariances for Differential Tip/Tilt Jitter (DTTJ, described in Section 2.1.1) and measurement error (Section 2.1.2). This procedure promotes stars with more secure positions and penalizes stars with noisy centroids.

2.3.1. Static Distortion Errors. It is assumed that the static distortion of the detector is known at the ~10 mas level through on-sky calibration techniques such as cluster observations (e.g., Anderson & King 2003[26]). The static

components of distortion of the Hubble Space Telescope Fine Guidance Sensor and the Keck AO NIRC2 narrow-camera have both been calibrated to better than 1 mas.[26,25] The dynamic component of the distortion due to instrumental flexure is assumed to be reduced to the microarcsecond level through the use of the diffractive pupil.[20]

3. RESULTS

3.1 Performance Trends with Telescope Diameter and Field of View

Here we use the Cameron et al. (2009)[12] technique to analytically predict the final astrometric performance of an 8-m MCAO system with a diffractive pupil as a function of telescope diameter and field size. The *K*-band Strehl is assumed to be 40% across the field of view and the pixel size is chosen to give Nyquist sampling in each case. For these cases, we assume that the primary target star has $K = 7$ and the total exposure time is 1 hour. Figure 4 plots the final single-axis, relative astrometric precision on the target star as a function of telescope diameter and field size for Galactic latitudes of $b = 20°$ and 90°.

At both Galactic latitudes plotted, the performance as a function of telescope diameter tends to flatten above diameters of D ~ 8 meters. This is due to the saturation of reference stars at increasingly faint limits as the aperture grows. The magnitude function of background stars begins to flatten at K ~ 20, so fewer reference star photons per star are available for D > 8 meters. The performance for D > 8 meters is determined by the choice of the exposure time of individual frames (3 seconds for this simulation). Reducing this exposure time of individual frames would improve the performance of larger telescopes, but lengthen the total exposure time substantially due to more readouts.

The principal advantage of MCAO here is the concentration of PSFs and the reduction of the star S/N term in the astrometric error budget. DTTJ error is the same as in a seeing-limited case due to the use of the diffractive pupil. We do not include the effects of PSF variation throughout the field in this simulation, although this effect is also mitigated by MCAO. Little improvement is seen by expanding the MCAO field diameter from 2 to 4 arcminutes, at least for D > 8 m, and a field of 1 arcminute is sufficient to attain ~10 microarcseconds relative astrometric precision per coordinate for D > 8 m.

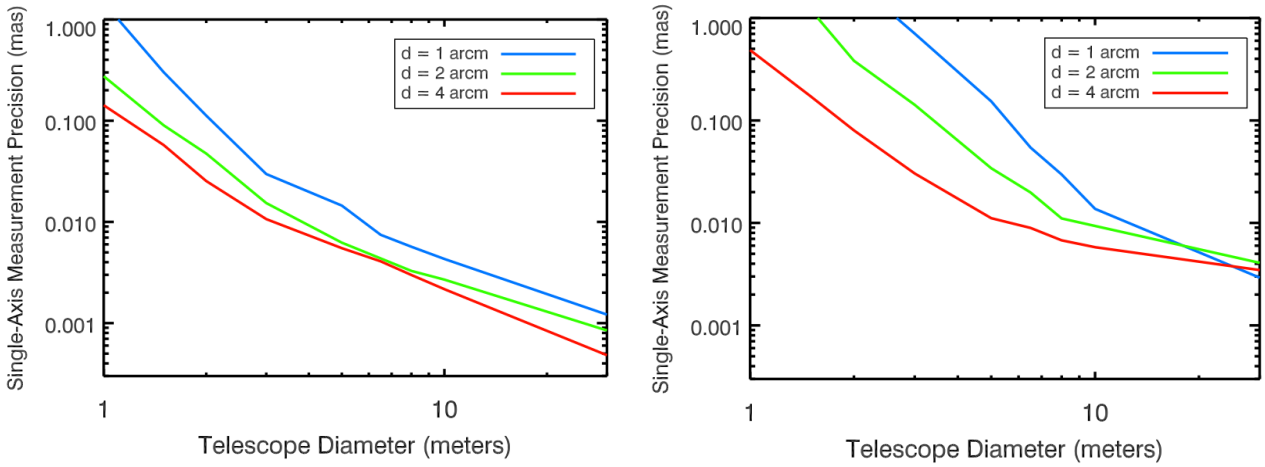

Fig. 4. Total relative astrometric error in milliarcseconds with MCAO as a function of telescope diameter. Colors denote different field diameters. *Left panel:* Galactic latitude of $b = 20°$. *Right panel:* Galactic latitude of $b = 90°$. The performance flattens as a function of diameter for D > 10 due to star saturation at fainter magnitudes with larger apertures.

4. SUMMARY

We have investigated the astrometric performance of an MCAO system equipped with a diffractive pupil using simplified MCAO simulations as well as an analytical, minimum-variance technique. MCAO presents a number of advantages for astrometry, including sharper PSFs, a uniform PSF distribution, and active cancellation of DTTJ. However, the out-of-pupil deformable mirrors in MCAO systems also introduce the possibility of systematic distortion changes on long time baselines. The diffractive pupil technique, in which star positions are referenced against

diffraction spikes generated by a grid of rods or dots at the first pupil, calibrates systematic changes in the distortion map and could potentially mitigate the problems inherent to MCAO.

A simplified MCAO simulation modeling the wavefronts of the diffraction spikes showed that the astrometric motions of the reference stars and the nearest diffraction spikes are decorrelated, such that the contribution of the atmosphere can be analytically modeled as the normal seeing-limited DTTJ error as described in Sasiela (2007).[23]

We then used the Cameron, Britton, & Kulkarni (2009)[12] weighting method with the full DTTJ equation and the star S/N term to simulate the idealized astrometric performance of an MCAO system equipped with a diffractive pupil. The performance was simulated as function of telescope diameter D, field diameter d, and Galactic latitude b for a target star of $K = 7$ and a total exposure time of 1 hour. The CDAR and ADAR errors were assumed to be reduced to the microarcsecond level through the use of atmospheric modeling techniques.[24] The sum of the atmospheric and measurement noise terms approached 4-6 microarcseconds for an 8-meter telescope with a 1 hour exposure. There does not appear to be a significant gain by increasing the field size from 2 to 4 arcminutes, especially for larger telescopes ($D > 8$ m), and a field diameter of 1 arcminute is sufficient to realize ~10 microarcseconds astrometric precision for $D > 8$ m.

5. ACKNOWLEDGEMENTS

Thanks to Matthew Britton, Jessica Lu, Ruslan Belikov, Quinn Konopacky, Brent Ellerbroek, Michael Hart, Luc Gilles, Matthias Schoeck, and Michael Shao for contributions and helpful discussions. Brent Ellerbroek and Matthias Schoeck are recognized for running simulations that inspired the MCAO simulations we publish in Section 2. We recognize support from the NASA APRA program. E.A.B. acknowledges support from the Fulbright Science and Technology program. S.M.A. acknowledges research support from the LLNL Lawrence Fellow program. This work performed under the auspices of the U.S. Department of Energy by Lawrence Livermore National Laboratory under Contract DE-AC52-07NA27344 with document release number LLNL-PROC-565933.

REFERENCES

[1] Sozzetti, A., "Detection and Characterization of Planetary Systems with μas Astrometry," EAS Publications Series, 42, 55 (2010).

[2] Shao, M., et al. "The Synergy of Direct Imaging and Astrometry for Orbit Determination of Exo-Earths," ApJ, 720, 357 (2010).

[3] Guyon, O., et al. "High-precision Astrometry with a Diffractive Pupil Telescope," ApJ, 2011, 11 (2012).

[4] Unwin, S., et al. "Precision astrometry with a space-based interferometer," proc. SPIE, 7013, 78 (2008).

[5] McBride, J., et al. "Experimental Design for the Gemini Planet Imager," PASP, 904, 692 (2011).

[6] Lu, J., et al., "Recent results and perspectives for precision astrometry and photometry with adaptive optics," proc. SPIE, 7736, 51 (2010).

[7] Majewski, S., et al. "Galactic Dynamics and Local Dark Matter," Chapter 4 of SIM Lite book, arXiv:0902.2759 (2009).

[8] Wehrle, A., et al. "Quasar Astrophysics," Chapter 11 of SIM Lite book, http://sim.jpl.nasa.gov (2009).

[9] Pravdo, S. & Shaklan, S. "Astrometric Detection of Extrasolar Planets: Results of a Feasibility Study with the Palomar 5 Meter Telescope," ApJ, 465, 264 (1996).

[10] Benedict, G.F., et al. “Interferometric Astrometry of Proxima Centauri and Barnard's Star Using HUBBLE SPACE TELESCOPE Fine Guidance Sensor 3: Detection Limits for Substellar Companions,” AJ, 118, 1086 (1999).

[11] Perryman, M., et al., “The Hipparcos Catalogue,” A&A, 323, 49 (1997).

[12] Cameron, P.B., Britton, M., & Kulkarni, S., “Precision Astrometry with Adaptive Optics,” ApJ, 137, 83 (2009).

[13] Muterspaugh, M., et al. “PHASES High-Precision Differential Astrometry of δ Equulei,” AJ, 130, 2866 (2005).

[14] Jordi, C., “The European Space Agency (GAIA) mission: exploring the Galaxy,” Proceedings of the conference "Astronomy with Megastructures. Joint science with E-ELT and SKA", Editors: I. Hook, D. Rigopoulou, S. Rawlings and A. Karastergiou, arXiv:1105.6166 (2011).

[15] Fritz, T., et al., “What is limiting near-infrared astrometry in the Galactic Center?” MNRAS, 401, 1177 (2010).

[16] Trippe, S., et al., “High-Precision Astrometry with MICADO at the European Extremely Large Telescope,” MNRAS, 402, 1126 (2010).

[17] Ammons, S. M., et al. “Microarcsecond relative astrometry from the ground with a diffractive pupil,” proc. SPIE, 8151, 25 (2011).

[18] Marcy, G. & Butler, R.P. “Precision radial velocities with an iodine absorption cell,” PASP, 104, 270 (1992).

[19] Butler, R.P., et al. “Attaining Doppler Precision of 3 m s^{-1}”, PASP, 108, 500 (1996).

[20] Guyon, O., et al., “Single aperture imaging astrometry with a diffracting pupil: application to exoplanet mass measurement with a small coronagraphic space telescope,” proc. SPIE, 7731, 71 (2010).

[21] Guyon, O., et al., “Diffractive pupil telescope for high-precision space astrometry,” proc. SPIE, 8151, 24 (2011).

[22] Bendek, E., et al., "Dynamic distortion calibration using a diffracting pupil: high precision astrometry laboratory demonstration for exoplanet detection," proc. SPIE, 8151, 26 (2011).

[23] Sasiela, R.J. [Electromagnetic Wave Propagation in Turbulence: Evaluation and Application of Mellin Transforms], 2nd edition, SPIE press, Bellingham, Washington, pp. 170-171 (2007).

[24] Gubler, J. & Tytler, D., “Differential Atmospheric Refraction and Limitations on the Relative Astrometric Accuracy of Large Telescopes,” PASP, 110, 738 (1998).

[25] Yelda, S., et al., “Improving Galactic Center Astrometry by Reducing the Effects of Geometric Distortion,” ApJ, 725, 331 (2010).

[26] Andersen, J. & King, I., “An Improved Distortion Solution for the Hubble Space Telescope's WFPC2,” PASP, 115, 113 (2003).

[27] Neichel, B. et al. “The Gemini MCAO System GeMS: nearing the end of a lab-story,” proc. SPIE, 7736, 4 (2010).

[28] Bahcall, J., & Soneira, R., “The universe at faint magnitudes. I - Models for the galaxy and the predicted star counts,” ApJS, 44, 73 (1980).